Ionosphere Spatial Gradient Threat for LAAS: Mitigation and Tolerable Threat Space

Ming Luo, Sam Pullen, Todd Walter, and Per Enge
Stanford University

ABSTRACT

The ionosphere spatial gradients under extreme conditions are likely to influence the LAAS architecture, particularly for Category II/III precision approach and landing systems. In previous study, a "moving wave front" model was established and a threat space was extrapolated based on the 6 April 2000 ionospheric storm. It was showed that the impact of the ionospheric anomalies depends on the threat parameters, namely, the ionospheric gradient, the slope width, and the wave front speed. Under a typical 24-satellite constellation, the maximum user vertical error at 5 km of user-to-LGF separation can reach as high as 20 meters in the worst case. However, with prompt detection of LAAS Ground Facility (LGF), the maximum user vertical position error can be mitigated to under 6 meters. Airborne monitor can further reduce the error especially when the ionospheric wave front moves fast. Although those work provided essential insights, due to the limited data available thus far and the uncertainty of the ionospheric storm behavior, many important questions remain unanswered: The prior probability of such extreme event, the conservativeness of the threat space, the creditability of the "moving wave front" model, etc.

In this study, the analysis was extended to less-ideal constellations, i.e, with one or two satellites outages. In addition to the "moving wave front" model, the focus was shifted to "stationary front" scenarios, which means that the ionospheric front stops moving prior to reaching the LGF. The impact of such scenarios is worse since LGF could not detect such an event by definition. It was found that the worst user error could reach 45 meters under extreme conditions. Although an airborne monitor can help to reduce the error significantly, the remaining maximum error can still be as high as 31 meters. While more data analysis effort are undergoing in order to refine the threat model, a parallel approach was undertaken to identify the system design vulnerability, i.e., to define a sub threat space that is tolerable for LAAS. It was found that under worst conditions, ionospheric stationary fronts with a slope of 70 mm/km or higher is not tolerable. The current airborne monitor does not help on increasing the tolerable threat space.

Although LGF and airborne detection are extremely important, the current architecture may not be able to meet LAAS requirements [3, 11, 12] under worst-case ionosphere conditions. Two means are examined for ionospheric threat mitigation: "Inner Satellites Protection" and Long Baseline Monitor (LBM). The effeteness of the outer satellites to protect the inner satellites is very limited particularly with fewer satellites in view. On other words, the inner satellites remain vulnerable for those worst cases. LBM is able to fully mitigate the problem for the entire threat space. The optimum LBM separation was recommended for consideration.

1.0 INTRODUCTION

The ionosphere is a dispersive medium located in the region of the upper atmosphere between about 50 km to about 1000 km above the earth [1]. The radiation of the sun produces free electrons and ions that cause phase advance and group delay to radio waves. As GPS signals traverse the ionosphere, they are delayed by an amount proportional to the total electron content (TEC). The state of the ionosphere is a function of intensity of solar activity, magnetic latitude, local time, and other factors. The error introduced by the ionosphere into the GPS signal is highly variable and difficult to model at the level of precision needed for LAAS. However, under nominal condition, the LAAS user differential error is small (less than 25 cm).

The possibility of extremely large ionosphere spatial gradients was originally discovered in the study of WAAS "supertruth" (post-processed, bias-corrected) data during ionosphere storm events at or near solar maximum (2000-2001). The sharpest gradient is 6 m over the IPP separation of 19 km (more detailed data analysis on this ionospheric event can be found in [2]). This gradient translates into an ionosphere delay rate of change of approximately 316 mm/km, which is 63.2 times the typical one-sigma ionosphere vertical gradient value identified previously. (A conservative one-sigma value for vertical ionosphere spatial decorrelation is about 5 mm/km [10]). Since a Gaussian extrapolation of the 5 mm/km one-sigma number does not come close to overbounding this extreme gradient, and because it is impractical to dramatically increase the broadcast one-sigma number without losing all system availability, we must treat this event as an anomaly and detect and exclude cases of it that lead to hazardous user errors.
Based on the WAAS supertruth data and available IGS/ CORS observations [2, 5], the iono anomaly is modeled as a semi-infinite "cloud" with a wave front. The gradient itself is simplified as a linear change in vertical ionosphere delay between the "high" and "low" delay

zones. The ionospheric slope and width are two parameters used to specify the gradient, as shown in Figure 1. The maximum ionospheric delay of the wave front (high-to-low vertical delay difference) is the product of the slope and the width. The "baseline" model directly extracted from 6 April 2000 WAAS supertruth data showed a slope of 316 mm/km, width of 19 km, and the maximum vertical delay of 6 m.

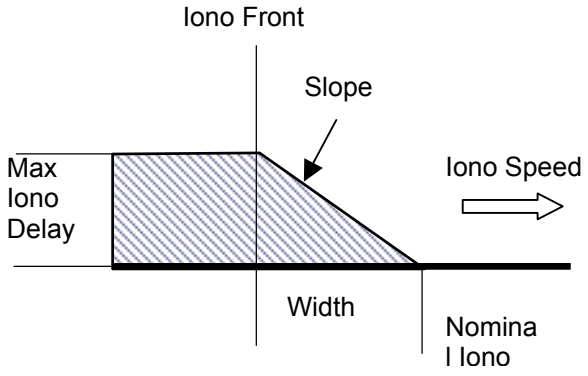

Figure 1: A simplified ionospheric wave front model

In order to better capture the range of possible ionosphere wave front characteristics, the linear gradient model shown as Figure 1 is redefined with three parameters: velocity, gradient width (w), and gradient slope (g). The total delay difference (D) is then given by: $D = wg$. Velocity includes both scalar speed ($|v|$) and direction. For direction, we define a velocity vector along the aircraft approach direction (the worst case from the last slide) as 0 degrees. While this linear model is an approximation of reality and is likely to be conservative, it provides a reasonable basis for sensitivity studies of the threat posed by a wide variety of potential ionosphere anomalies. Obviously 0 degree represents the worst angle between the front moving and the airplane approaching.

Based on the anomaly data analyzed thus far, a threat space has been developed by the LAAS Key Technical Advisors to identify the upper and lower bounds on each of the variables in the threat space, as shown in Figure 2. For the gradient slope, the lower bound of 30 mm/km represents 6 times the one-sigma value expected in CONUS during active ionosphere periods (5 mm/km), and the upper bound represents a hypothetical 6 meters of vertical delay difference over the minimum gradient width of 15 km. Note that there is an external constraint that the total vertical ionosphere delay difference D must be no greater than 10 meters (the maximum delay difference considered possible over the short baselines considered here). Thus, points nominally within the 3-D hypercube of this threat space that have $wg > 10$ m are excluded from the threat space. This threat space is used in all of the simulation results in this paper.

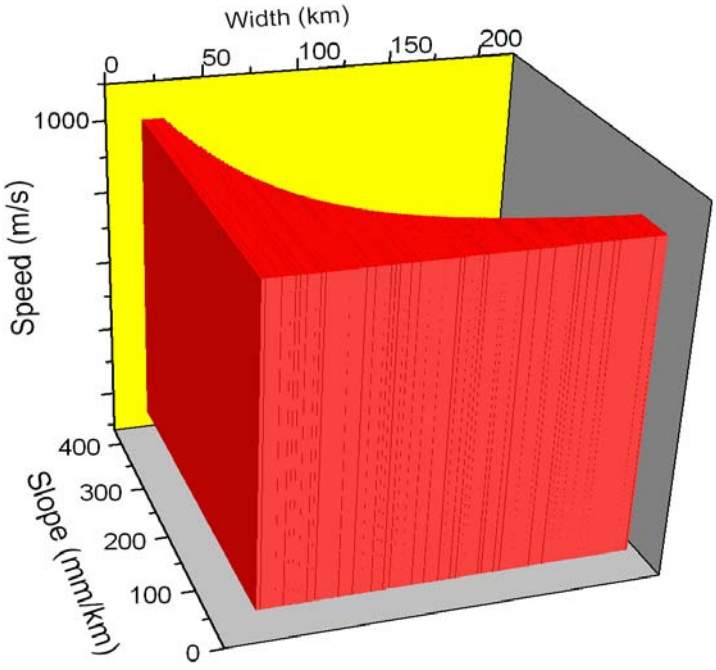

Current Threat Space:

Width: 15 – 200 km

Slope: 30 – 400 mm/km

Speed: 0 – 1000 m/s

Constraint :
***Max Delay* ≤ 10 m**

Figure 2: Ionosphere Spatial Anomaly Threat Space

Study of ionosphere data for other known ionospheric storm days is underway to attempt to better define the threat model. In the meantime, the full threat model is used in the simulations reported in this paper. Note that the threat model definition also constrains the total amplitude (slope × width) of the vertical ionospheric delay gradient to be no greater than 10 meters. The points on the slope and width plot that translate into total delays exceeding 10-meters are not part of the threat model, ("cut out" as included in this plot).

2.0 PREVIOUS STUDY REVIEW

In this chapter, several key previous works will be reviewed briefly including the simulation methodology, basic assumptions, LGF and airborne monitoring models. The detailed description can be found at [9].

2.1 Position Domain Simulation

It is important to estimate the impact of ionospheric anomaly on LAAS users. If both the user and the LAAS LGF observe the same ionospheric delay on a given GPS satellite, then there is no impact since the user error induced by the ionosphere will cancel out when the differential corrections broadcast by the LGF are applied. However, if the user and the LGF see different ionosphere delays, there will be some differential error. Given that this wave sweeps over a LAAS-equipped airport, the worst case from the aircraft's point of view is a wave front that approaches from directly behind an aircraft on approach and overtakes the ionospheric pierce point of an aircraft before the aircraft reaches its decision height. (A typical jet aircraft final approach speed is about 70 m/s). After the wave front overtakes the aircraft, a differential range error builds up as a function of the rate of overtaking and the slope of the gradient. Before the wave front reaches the corresponding LGF pierce point, there is no way for the LGF to observe (and thus be able to detect and exclude) the anomaly. The worst-case timing is that which leads to the maximum differential error (often this means the time immediately before LGF detection and exclusion) at the moment when the aircraft reaches the decision height for a particular approach (the point at which the tightest VAL applies). Note that this worst-case event and timing, if it ever were to occur, would only affect one aircraft. Other aircraft on the same approach would be spread out such that the wave front passage would create no significant hazard for them (VAL far from the decision height is higher than the error that could result from this anomaly [11]).

A "moving wave front" of this sort is sketched in Figure 3. In this scenario, the user is 45 km away (the limit of LAAS VHF data broadcast coverage [3]) and is approaching the LGF at a speed of 70 m/s. The ionosphere front is behind the airplane and is moving in the same direction at a speed of 110 m/s. The ionosphere front is going to "catch" the airplane (reach the IPP between the aircraft and the GPS satellite), pass it, and eventually hit the IPP between the LGF and the satellite. The LGF "sees" the ionosphere from then on and gradually incorporates it into its differential corrections. The impact of this baseline ionosphere anomaly model on LAAS users was analyzed in detail in [4]. A sensitivity study can also be found in the same paper.

In order to translate range-domain errors into position errors, a simulation has been conducted using the satellite geometry visible at Washington, D.C. at the time of passage of the ionosphere anomaly on 6 April 2000. Although it will not necessarily apply to all such anomalies, it is assumed that the wave front in this case moved approximately from North to South. The scenario is illustrated with the sky plot in Figure 3.

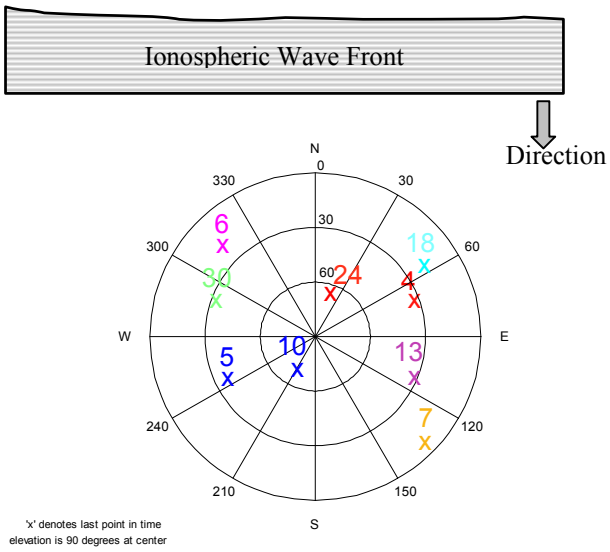

Figure 3: Illustration of Satellite Geometry and Ionospheric Motion

For each fixed satellite geometry, we let the ionospheric wave front move from the very north to the very south of the "sky". Only the thin shell ionospheric model is used in the simulation; and the height of the shell is assumed to be 350 km above the surface of the earth. It can be calculated that the distance that the wave front travels is about 4235 km. Each satellite IPP is going to be "hit" by the wave front; one after another. Then the satellite geometry propagates to the next step (in a 10-minute interval), and the wave front sweeps through the "sky" again. Thus, all combinations of satellite geometry in 24 hours and the ionospheric wave front location are considered.

Figure 4 illustrates the vertical position error for the baseline wave front case. The *x*-axis is the location of the ionospheric wave front. The *y*-axis is the user vertical position error. As can be seen, whenever a satellite IPP is hit, there is a peak of vertical error associated with it. Note that the height of the peak depends on which satellite is impacted and when it is impacted.

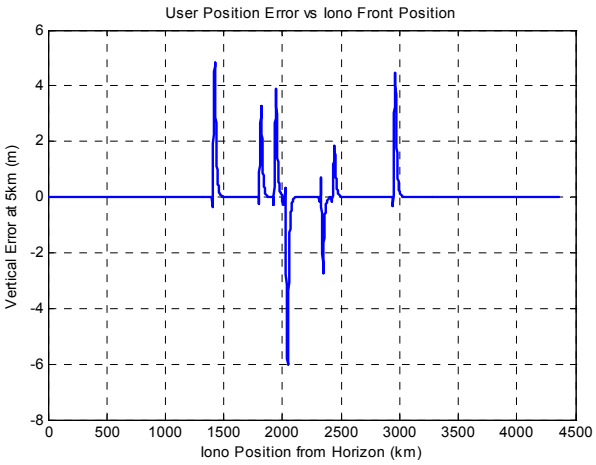

Figure 4: Illustration of Vertical Position Error with Iono Front "sweeps across" the sky

2.2 LGF and Airborne Monitoring

When the ionosphere wave front moves toward the airport, the LGF will be affected by the ionosphere front at some point during an approach. Once it is affected, one or more of the existing LGF integrity monitors may issue an alert despite not being designed specifically to detect this anomaly. In order to quantify this, we used the Stanford Integrity Monitor Testbed (IMT), an LGF prototype developed at Stanford University, to simulate the detection ability of the LGF. The IMT consists of various monitors to address integrity concerns such as satellite signal failures, ephemeris anomalies, receiver problems, RF interference, etc. Though each monitor was designed to target different failure modes, it was found that multiple monitors of the IMT can detect the ionosphere spatial gradient modeled here. Among them, MQM (Measurement Quality Monitoring) is the fastest to detect relatively large ionospheric change rate. CUSUM (The Cumulative Sum) is the most effective on detecting small but hazardous ionospheric gradients. For airborne monitor, a traditional GMA (Geometric Moving Averaging) code-carrier divergence monitor is used in the analysis. A detailed IMT descriptions and algorithms can be found in [6,7,8].

Since each IMT monitor was designed to target different potential failure modes in LGF measurements, their times-to-detect vary with apparent ionospheric delay rate-of-change as well as elevation angle. An example failure test is shown in Figure 5. The overall time-to-detect by the LGF is shown as the blue line (circles). As can be seen, MQM is the fastest when the apparent ionospheric rate is above a certain level (e.g., greater than 0.02 m/s for a high-elevation-angle satellite), and the CUSUM code-carrier divergence method is the best when the ionospheric rate is lower than this but still anomalous (e.g., between 0.01 and 0.02 m/s). For this analysis, it is assumed that no monitor detects ionosphere events with apparent ionosphere delay rates-of-change at the LGF lower than 0.01 m/s (this is likely required to meet the LGF continuity sub-allocation during non-hazardous ionosphere storms). Clearly, MQM and CUSUM method together give the best possible lower bounds on detection time. The time-to-detect for the airborne is also plotted in the same plot in red assuming that only the GMA algorithm is used there and that its performance is roughly equivalent to ground-based GMA. For any given ionospheric gradient greater than 0.035 m/s, it takes significantly longer time for the airborne to detect than for the LGF. Note that these test results may be strongly associated with factors unique to the Stanford IMT such as siting, antenna type, etc. The value used here may need to be adjusted to suit a different LGF system design.

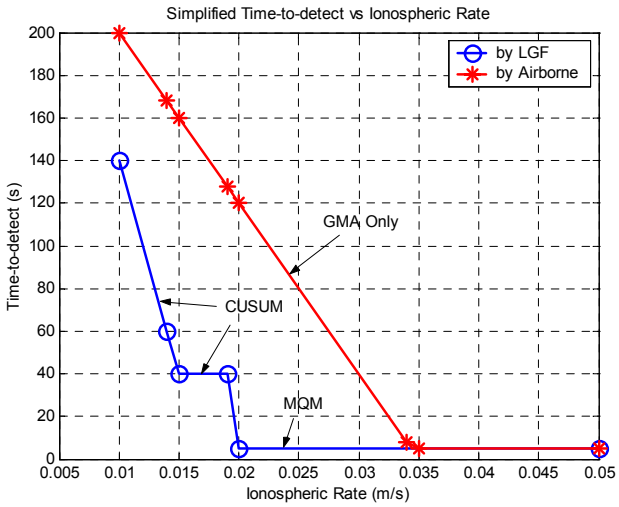

Figure 5: Time-to-detect vs. Ionosphere Delay Rate of Change (from Stanford IMT Failure Testing)

3.0 MOVING WAVE FRONT SCENARIOS

3.1 Impact for 24 SVs Constellation

For each fixed satellite geometry and given ionospheric threat, the simulation gives a result in the format of Figure 4. After a set of geometries of interest is cycled through (e.g., for 24 hours at DC with 10 minutes interval), a maximum vertical error can be found for that

given ionospheric threat. After the process is repeated for every point within the threat space, then all the maximums through the entire threat space are collected and put in Figure 6. In other words, the points on these plots represent the impact of the ionosphere wave for the worst satellite affected and at the worst time during the 24 hours. Each column represents a different wave front speed ranging from 100 m/s to 900 m/s. No monitoring, LGF monitoring, and both LGF and airborne monitoring are shown in red (row 1), blue (row 2), and green (row 3), respectively. The maximum vertical errors are about 20, 6, and 5 meters for the three monitoring categories. Generally, the faster the wave front speeds, the smaller the vertical error. LGF and airborne monitors both help on mitigating the threat significantly. But each monitor has different advantages and disadvantages: LGF monitors have better algorithm, sees higher relative rate of ionospheric gradient change, therefore the time-to-detect us shorter (as shown in Figure 5). However, in the moving scenarios LAAS worries the most (wave front "chasing" the airplane from behind), the user always sees the wave front before the LGF, so the airborne has a chance to detect the anomaly earlier, particularly for fast moving wave fronts.

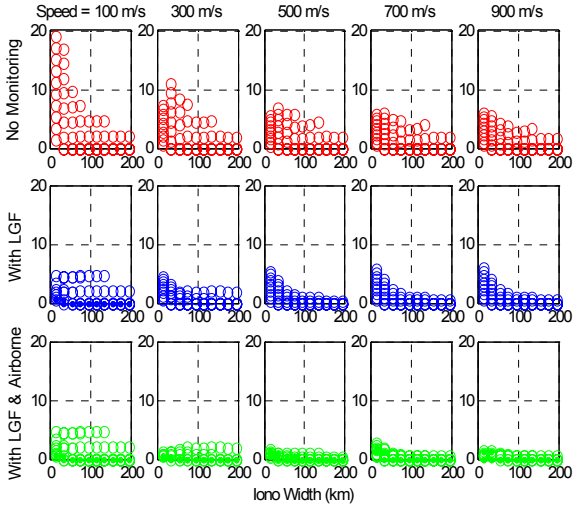

Figure 6: Summary of Maximum Vertical Errors for 24-SV Constellation

3.2 Impact with Satellite Outages

Although the maximum errors are reduced under 6 meters with LGF and airborne monitors in place for typical 24 satellites constellation, it is important to find out the ionospheric impact with satellite outages. Figure 7 and 8 showed the summary plots for 23 SVs and 22 SVs constellation, respectively. As can be seen, with 1 satellite outage (23 SVs constellation), the maximum error reaches 35 meters without monitoring. With LGF alone or with both LGF and airborne monitoring, the errors are mitigated under 10 meters. With 2 satellites outage, the error goes as high as 45 meters without monitoring. Even with both LGF and airborne monitors, the remaining errors can still be over 10 meters (11.5 meters). Recall that VAL (the Vertical Alert Limit) is set to be 10 meters for Cat I LAAS. An error caused by ionospheric anomaly alone over 10 m is obviously intolerable.

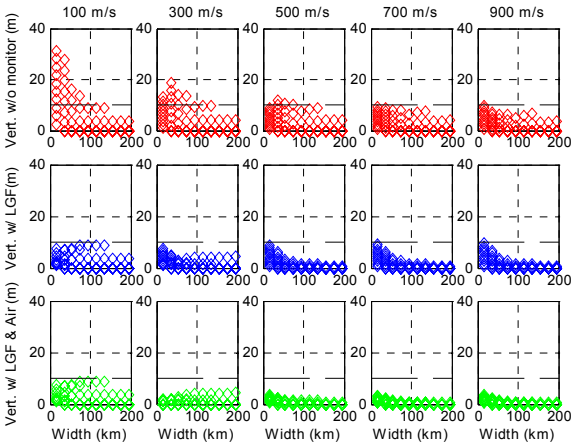

Figure 7: Summary of Maximum Vertical Errors for 23-SV Constellation

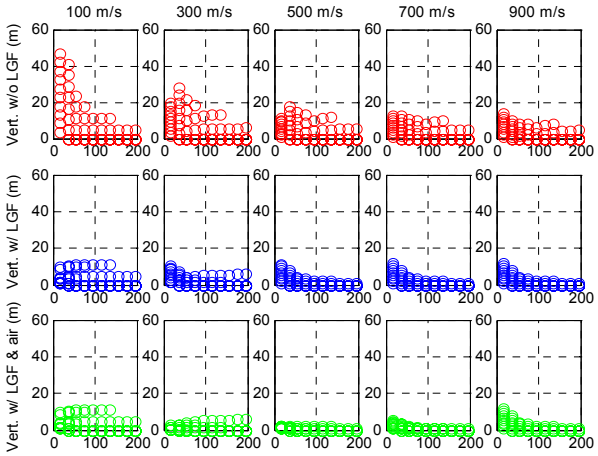

Figure 8: Summary of Maximum Vertical Errors for 22-SV Constellation

It is very desirable to bring the residual error under VAL. There is one parameter one can adjust in the broadcasted message: σ_{vig}, which is the one-sigma vertical ionospheric spatial gradient under nominal condition. The current setting of σ_{vig} is 5 mm/km. It was found that if σ_{vig} is adjusted to be 10 mm/km instead, then all the

residual error would be brought down under 10 meters. The tradeoff is that more geometries would be marked as "unavailable" in that case.

4.0 STATIONARY FRONT SCENARIOS

Since the general tread indicates (as Figure 6 – 8) that the slower wave front would have more severe impact on a LAAS user, it is natural to focus on the extreme case: a stationary wave. In the threat space shown as Figure 2, it means the 2-dimention "wedge" on the very bottom of the "cube". In practice, it means a wave front stops moving before reaching the LGF. By definition, LGF would not be able to detect such an event. A stationary front scenario is sketched as Figure 9. Note that the user is not only going to suffer the differential error at the moment of reaching the decision height, but also carry the history due to carrier smoothing process. The actual portion of the ramp that causes the differential error is indicated as a red bar in the figure.

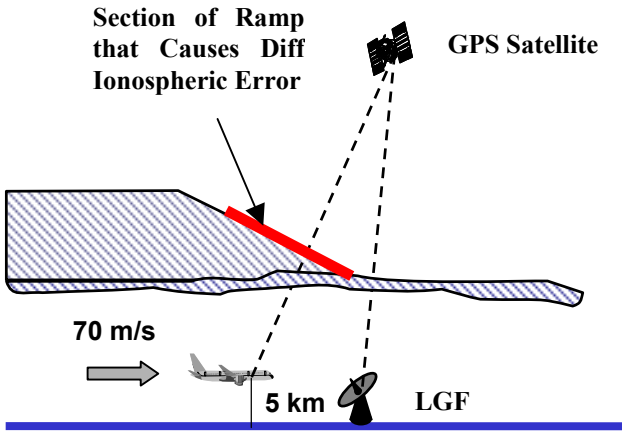

Figure 9: Illustration of Stationary Front Scenarios

The differential range error would then become: Slope * min{ (5 + 2 τ * v_air), width}. Where v_air is the speed of airplane approaching, 5 km is associated with the decision height, and τ is the carrier smoothing time constant. In other words, if the width is small, then the entire ramp will contribute to the differential error. If the width is large, than only one portion of it will be effective on inducing error.

Figure 10 shows the maximum vertical error for 24 SVs constellation under stationary front scenarios. Each curve represents an ionospheric front slope while the *x*-axis is the front width. As expected, the greater the slope, the bigger the error. And as long as width is greater than 30 km or so, the error stays constant. That is because the "effective" portion of the ramp remains the same even as the ramp becomes wider. The maximum error in this case is about 16 meters. It can also be read from this figure that an ionospheric front with slope of less than 170 mm/km will not cause a vertical error greater than 10 meters.

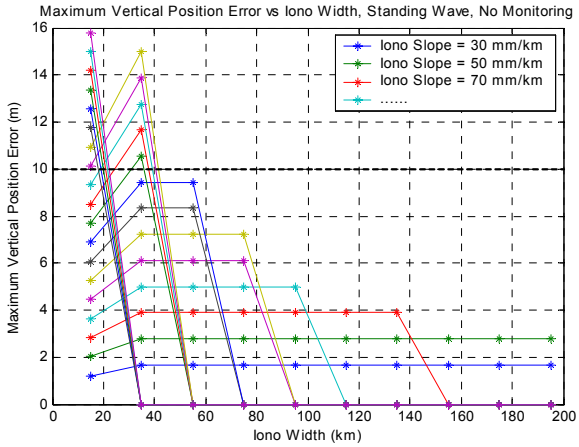

Figure 10: Maximum Error for Stationary Wave Front, 22-SV Constellation

The analysis was extended to cover all the 24-SV, 23-SV, and 22-SV constellations. The effeteness of the airborne monitoring and the impact of σ_{vig} are all included in the study. Figure 11 shows an example results for 22-SV constellations. As can be seen, both airborne monitor and σ_{vig} reduces the maximum error significantly. However, even with all the mitigation tools in place, the remaining error still reaches as high as 20 meters.

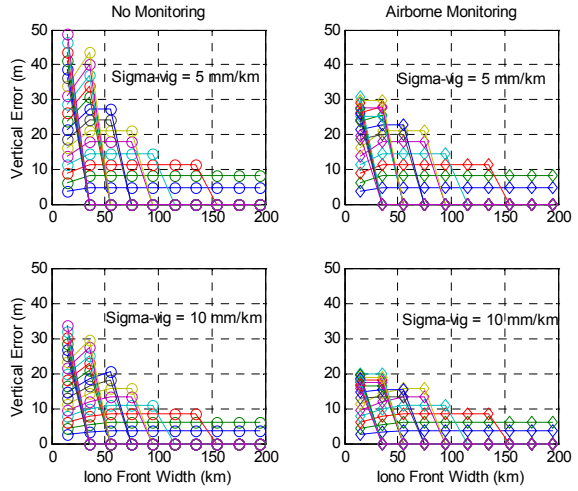

Figure 11: Maximum Error for Stationary Wave Front, 22-SV Constellation

The maximum errors for all the cases studied are summarized in Table 1. The red region indicates errors greater than 10 m and the green regions represent error less than 10 m. Clearly, stationary front scenarios are worse than moving wave front cases by a big margin. Even with airborne monitor and σ_{vig} adjusted, the residual error is still over 10m, i.e, in "red".

Table 1: Summary Table of Maximum Vertical Errors

Monitoring Category	Moving Wave Front				Stationary Front Scenarios				
	24 SVs	23 SVs	22 SVs		24 SVs	23 SVs		22 SVs	
	σ_{vig} = 5 mm/km	σ_{vig} = 5 mm/km	σ_{vig} = 5 mm/km	σ_{vig} = 10 mm/km	σ_{vig} = 5 mm/km	σ_{vig} = 5 mm/km	σ_{vig} = 10 mm/km	σ_{vig} = 5 mm/km	σ_{vig} = 10 mm/km
No Monitoring	20 m	30 m	45 m	30 m	16 m	40 m	27 m	49 m	35 m
LGF Monitoring	6 m	10 m	11.5 m	10 m	NA	NA	NA	NA	NA
Airborne Monitoring	5 m	10 m	11.5 m	10 m	11 m	25 m	20 m	31 m	20 m

5.0 "TOLERABLE" SPACE FOR LAAS

Knowing the magnitude of the ionospheric impact and its dependence on the threat parameters, it would be very helpful to refine the threat model. However, the data processing is very time consuming. While more data analysis effort are undergoing in order to refine the threat model, a parallel approach was undertaken to identify the system design vulnerability, i.e., to define a sub threat space that is tolerable for LAAS. Every point in Figure 10 can be read and re-plot in the 2D threat space (focused on stationary front scenarios only) shown as Figure 12. For any given threat (a combination of the front slope and width), if the maximum error exceeds 10 m, plot it read. Otherwise draw a green star. The green area therefore would indicate the threat space that is associated with errors less than 10 m, which is denoted as "tolerable". As can be seen, for 24 SVs constellation without airborne monitoring, the "tolerable area is slope ≤170 mm/km, or slope ≤ 230 mm/km and width ≤ 15 km.

Figure 13 showed the comparison of "tolerable" space with and without airborne monitoring, and using ≤ of 5 mm/km or 10 mm/km. Note that although airborne monitor and both help on reducing the maximum error (as shown on Figure 11), they don't help on increasing the "tolerable space" by much. The reason is that the error are reduced by the mitigations means, but not sufficient to bring it under 10 m. The tolerable spaces for all scenarios studied in this paper are summarized in Table 2. Red indicates a low tolerance (small gradient slope), green means a reasonable tolerance, and yellow are marginal.

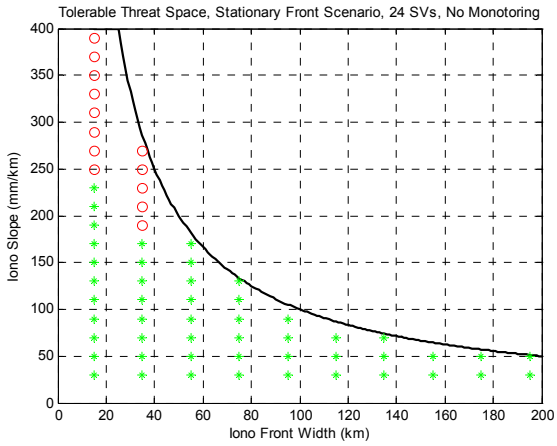

Figure 12: "Tolerable" Space For Stationary Front Scenarios, 24-SV Constellation, No Monitoring

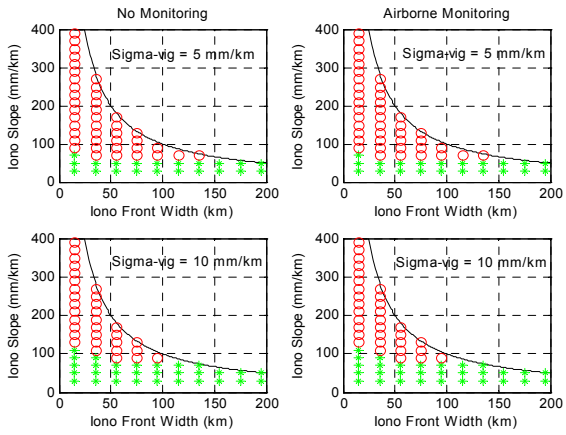

Figure 13: "Tolerable" Threat Space For Stationary Front Scenarios, 22-SV Constellation

Table 2: "Tolerable" Threat Space For Stationary

Monitoring Category	Moving Wave Front				Stationary Front Scenarios				
	24 SVs	23 SV3	22 SVs		24 SVs	23 SV3		22 SV3	
	σ_{vig} = 5 mm/km	σ_{vig} = 5 mm/km	σ_{vig} = 5 mm/km	σ_{vig} = 10 mm/km	σ_{vig} = 5 mm/km	σ_{vig} = 5 mm/km	σ_{vig} = 10 mm/km	σ_{vig} = 5 mm/km	σ_{vig} = 10 mm/km
No Monitoring	Speed Dependent (Worse for Lower Speed)				≤ 170 mm/km	≤ 70 mm/km	≤ 90 mm/km	≤ 50 mm/km	≤ 70 mm/km
LGF Monitoring	All	All	Speed dependent	All	NA	NA	NA	NA	NA
Airborne Monitoring	All	All	Speed dependent	All	≤ 230 mm/km	≤ 70 mm/km	≤ 90 mm/km	≤ 50 mm/km	≤ 70 mm/km

6.0 MITIGATION

The results shown thus far that the error caused by such an ionospheric anomaly can be severe and the monitoring means currently in place is not effective enough. In order to fully protect the user under this threat, further mitigation need to be considered.

6.1 "Outer" SVs Protect "Inner" SVs

Although it might be possible for the ionospheric front suddenly emerge and disappear in the middle of nowhere, it seems more likely that the large gradient portion formed at one place and move to other places. In the scenario shown as Figure 3, the satellite on the north "edge" (SV 6 for this particular sky view) would be impacted first before other satellites. If the LGF has a smart logic built in to stop further broadcasting after the first one or two satellites are impacted, then no further can be induced to the user (again, the trade off is the loss of availability). To extend the idea to a more general case, say the ionospheric front can sweep in from any direction (instead of north as Figure 3), whatever it is from, the satellites at the edge of that particular direction could possibly protect other satellites further down the path. The essence is that those "outer" satellites (typically with lower elevation angle) can probably protect those "inner" satellites (with higher elevation angle). If all directions are considered, the idea is sketched as Figure 14. In this case, SV 6, SV 18, SV 7, SV 5, and SV 30 belong to the "outer" group and SV 24, SV 4, SV 13, and SV 10 are "inner" satellites. As a result, the user error for a given geometry will have less peaks than previously illustrated as Figure 4. (The center peaks induced by those "inner satellites" are gone. It was found that with nine satellites in view for a typical 24-SVs constellation, the maximum error is reduced by 20%.

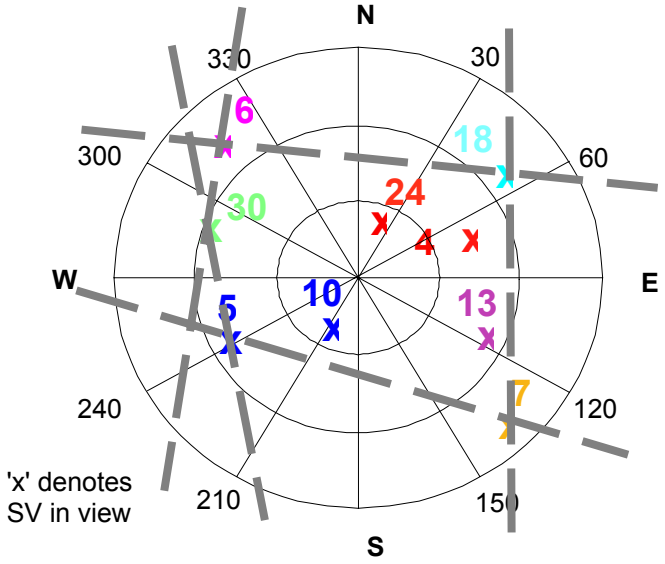

Figure 14: "Outer" SVs vs. "Inner" SVs, 9 SVs in View for a 24 SVs Constellation

As shown before, the more concerning cases are those of satellite outages. Take 22 SVs constellation as an example, a typical sky view with six satellites is shown as Figure 15. In this case, every satellite is an "outer" satellite therefore no "inner" satellite can be protected by this means. When searching through all 184 bad geometries with 2 SVs outage, "inner" satellites can be found in only two of those geometries. This method seems fail to mitigate ionospheric threat for those cases that needed the most. However, since fewer satellites are affected with this method given the wave front moves from any fixed direction, it help to reduce the overall probability (by a factor of 5 or so) of severe impact.

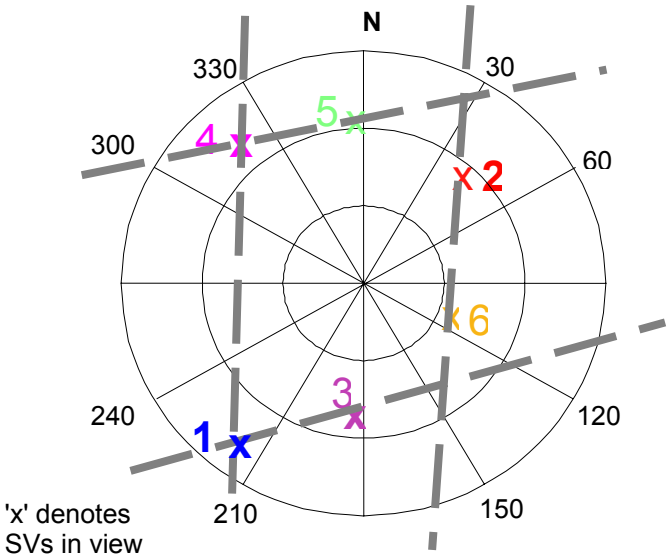

Figure 15: "Outer" SVs vs. "Inner" SVs, 6 SVs in View for a 22 SVs Constellation

6.2 Long Baseline Monitor (LBM)

A single baseline along the direction of the runway is illustrated as Figure 16. (Orthogonal baselines are probably needed for all runways.)

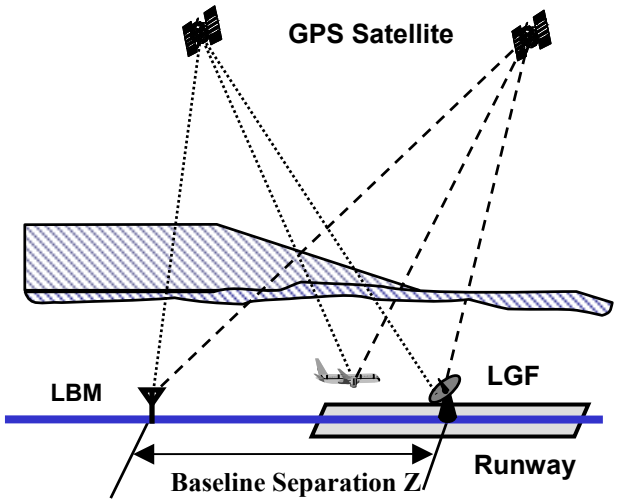

Figure 16: Illustration of Long Baseline Monitor

Double difference carrier residual can be used to observe and detect ionospheric anomalies. Derived from previous work on basic concept of Minimum Detectable Error (MDE) [13], it can be derived that for a LBM:

$$MDE = K_{ffd} \times K_{md} \times \sqrt{(\sigma_{LBM}{}^2 + (\sigma_{vig} \times Z \times F_{PP})^2}$$

Where:

MDE – Minimum Detectable Error
K_{ffd} – Fault Free K factor = 6.1
K_{md} – Missed Detection K Factor = 3.8
σ_{LBM} – One Sigma of LBM = 5 - 25 mm
σ_{vig} – One Sigma of Vertical Ionospheric Gradient = 5 mm/km
Z – LBM Separation from the LGF
F_{PP}– Obliquity Factor

Note that MDE consists of two parts: the sensitivity of the LBM (σ_{LBM}), and the nominal vertical ionospheric gradient () multiply by the separation Z. As expected, the smaller the σ_{LBM}, the more sensitive the LBM. On another hand, the longer the baseline is, the bigger the MDE becomes. A range of σ_{LBM} from 5 mm to 25 mm is considered in this study.

Now the entire ionospheric threat space is revisited again with LBM in place. The stationary front scenarios are the focus since it poses greater threat to LAAS users. The residual errors with various LBM separations are shown as Figure 17. When LBM is set 5 km away (the upper left sub-plot), the residual error is about the same as without LBM (see Figure 11 without monitoring case). When LBM is set farther and away, the residual error is reduced more and more effectively.

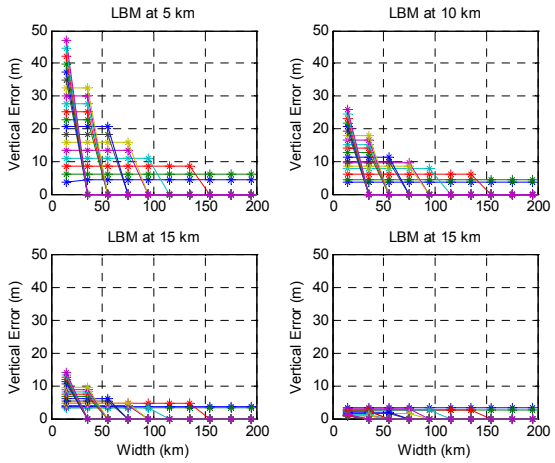

Figure 17: Maximum User Vertical Error with LBM of Various Baseline Separation

A more complete analysis is conducted and the maximum residual error is plotted against the LBM separation as shown in the upper sub-plot of Figure18. It shows that the residual error decreases when LBM separation increases within 20 km or so. Then it changes course and increases when LBM separation increases. The reason is that MDE increases with Z where the nominal gradient dominates. The lower subplot showed MDEs vs. Z for a group of satellites in view. For system design purpose, the proper range of LBM setting is

between 16 m and 60 m, with 20 m to be optimum separation. Note that theses results will change if the ionospheric threat space changes. It is also found the results are insensitive to because again, the nominal gradient dominates.

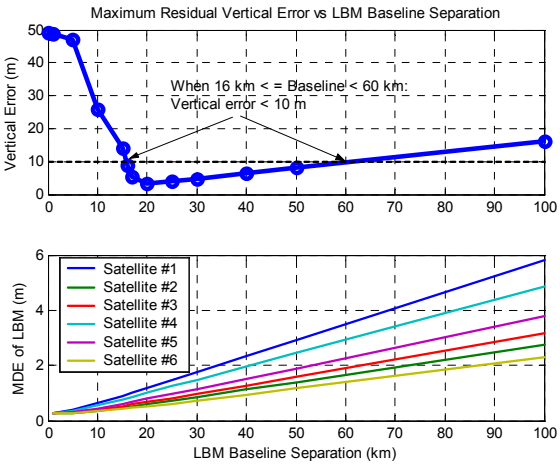

Figure 18: Maximum Vertical Error vs. LBM Baseline Separation

7.0 CONCLUSIONS AND ONGOING WORK

The impact of an ionospheric threat to LAAS is a strong function of threat model parameters (slope, width, and speed) and satellite geometry. For moving wave front scenarios, without any monitoring, the maximum vertical error is about 20 m for a 24-SV geometry and 45 m for a typical 22-SV geometry. With LGF and airborne monitoring, the residual error can be reduced to about 6 m. However, the impact of the worst stationary front scenarios is found to be more severe. The LGF is not able to detect such an event by definition. Even with airborne monitoring, the remaining error can still be as high as 31 m. A parallel approach was undertaken to identify the system design vulnerability, i.e., to define a subset of threat space that is tolerable for LAAS. Under worst conditions, ionospheric stationary fronts with a slope of 70 mm/km or higher are not tolerable. The current airborne monitor does not help on increasing the tolerable threat space. Under bad geometries and stationary front conditions, anomalous ionospheric gradient slopes above 70 - 90 mm/km are problematic, even with σ_{vig} = 10 mm/km.

LGF and airborne detection are extremely important. But the current architecture may not be able to meet LAAS requirements under worst-case ionosphere conditions. Two means are examined for potential ionospheric threat mitigation. The effectiveness of using outer satellites to protect inner satellites is very limited, particularly with fewer satellites in view. The Long Baseline Monitor (LBM) is able to fully mitigate the problem for the entire threat space if the LBM-to-LGF separation is set around 20 km.

The ongoing effort to better understand and mitigate the ionosphere spatial anomaly threat can be divided into two parts. The first part is to perform data analysis to better determine the credibility of the ionosphere spatial anomaly threat space and the relative likelihood of anomalies within this space. In order to achieve this goal, both recent CONUS ionospheric storms (using IGS data) and similar events in Japan (using the very dense Japan Geodetics reference station network known as GEONET) will be studied. The current version of the ionosphere threat model is very broad, and our approach has been to be conservative. With more data analysis, it may be possible to exclude physically unrealistic points from the threat model in the future (thereby creating a "reduced" threat model). However, since we will never have perfect physical information about the possible extent of ionosphere anomalies, the upper bounds on ionosphere gradients will remain somewhat arbitrary. The second part is to investigate further mitigation means of LAAS mitigation. Among them, improved airborne monitoring seems to be the most promising. The current model of airborne code-minus-carrier monitor performance is based on the IMT GMA monitor and is probably conservative – a monitor optimized for airborne use will likely have estimation filter time constant shorter than 200 seconds. Airborne monitoring is likely necessary for Category II/III approaches, depending on the VAL that is selected.

ACKNOWLEDGMENTS

The authors would like to thank the FAA LAAS Program Office (AND-710) for its support of this research. The opinions expressed here are those of the authors and do not necessarily represent those of the FAA or other affiliated agencies.

REFERENCES

[1] P. Misra, P. Enge, *Global Positioning System: Signals, Measurements, and Performance*. Ganga-Jamuna Press, 2001.

[2] S. Datta-Barua, *et.al*., "Using WAAS Ionospheric Data to Estimate LAAS Short Baseline Gradients," *Proceedings of ION 2002 National Technical Meeting*. Anaheim, CA, January 28-30, 2002, pp. 523-530.

[3] *Specification: Performance Type One Local Area Augmentation System Ground Facility.* Washington, D.C., Federal Aviation Administration, FAA-E-2937A, April 17, 2002.

[4] M. Luo, *et.al*, "Assessment of Ionospheric Impact on LAAS Using WAAS Supertruth Data", *Proceedings of*

The ION 58th Annual Meeting. Albuquerque, NM, June 24-26, 2002, pp. 175-186.

[5] T. Dehel, "Ionospheric Wall Observations," Atlantic City, N.J., William J. Hughes FAA Technical Center, FAA ACT-360, February 24, 2003.

[6] G. Xie, *et.al*., "Integrity Design and Updated Test Results for the Stanford LAAS Integrity Monitor Testbed (IMT)," *Proceedings of ION 2001 Annual Meeting*. Albuquerque, NM, June 11-13, 2001, pp. 681-693.

[7] B. Pervan, "A Review of LGF Code-Carrier Divergence Issues", Illinois Institute of Technology, MMAE Dept., May 29, 2001.

[8] G. Xie, *et.al.*, "Detecting Ionospheric Gradients with the Cumulative Sum (CUSUM) Method," Paper AIAA 2003-2415, *Proceedings of 21st International Communications Satellite Systems Conference*, Yokohama, Japan, April 16-19, 2003.

[9] M. Luo, *et.al*., "LAAS Ionosphere Spatial Gradient Threat Model and Impact of LGF and Airborne Monitoring", *Proceedings of ION GPS 2003*, Portland, Oregon., Sept. 9-12, 2003.

[10] S. Pullen, "Summary of Ionosphere Impact on PT 1 LAAS: Performance and Mitigation Options," Stanford University, Dept. of Aero/Astro, December 14, 2000.

[11] *Minimum Aviation System Performance Standards for Local Area Augmentation System (LAAS)*. Washington, D.C., RTCA SC-159, WG-4A, DO-245, Sept. 28, 1998.

[12] *Minimum Operational Performance Standards for GPS/Local Area Augmentation System Airborne Equipment*. Washington, D.C., RTCA SC-159, WG-4A, DO-253A, Nov. 28, 2001.

[13] S. Pullen, T. Walter, P. Enge, "System Overview, Recent Developments, and Future Outlook for WAAS and LAAS," *Proceedings of GPS Symposium 2002*. Tokyo, Japan, GPS Society/Japan Institute of Navigation, Nov. 11-13, 2002, pp. 45-56. http://waas.stanford.edu/~wwu/papers/gps/PDF/PullenTokyo02.pdf